

Crystal Growth of the Nanoporous Metal–Organic Framework HKUST-1 Revealed by In Situ Atomic Force Microscopy**

Maryiam Shoaee, Michael W. Anderson, and Martin P. Attfield*

Crystalline nanoporous materials are one of the most important groups of solid-state material with widespread utilization in a host of applications.^[1] The successful development and application of these materials will be greatly facilitated through a full understanding of the crystal growth mechanism. This will permit control of properties such as composition, structure, size, morphology, and the presence and form of defects within the crystals. As the product of the crystallisation process is determined by the process parameters themselves, the investigation and understanding of this process is of comparable importance to the correct choice of the reagents.^[2] Atomic force microscopy (AFM) is a technique that permits detailed observation of nanometer-sized features on crystal surfaces and unique insight into crystal growth processes through ex situ and in situ studies.^[3] Hitherto the application of AFM to the understanding of crystal growth of crystalline nanoporous materials has been limited to conclusions drawn from ex situ studies of crystal surfaces and in situ studies of crystal dissolution.^[4] In situ AFM studies of the crystal growth of this type of material are required to present definitive real-time evidence for the mechanism and to provide information on the nature of the fundamental structural units attaching to the crystal surface during growth. The latter can be related to the likely involvement of specific aggregates or secondary building units (SBUs) in the growth solution, one of the central questions in the synthesis of nanoporous materials.^[5] Here we present such evidence obtained from the first high-resolution in situ AFM study of the crystal growth of a crystalline nanoporous material, HKUST-1. This information will aid in the understanding of the mechanism of the reaction–crystallization processes that result in the formation of extended datively or covalently bound materials.

The copper trimesate $\text{Cu}_3[(\text{O}_2\text{C})_3\text{C}_6\text{H}_3]_2(\text{H}_2\text{O})_3$ (HKUST-1)^[6] is an important crystalline nanoporous metal–organic framework (MOF) that is receiving considerable interest in a variety of areas including the development of oriented membranes, and gas storage and purification.^[7–10] HKUST-1

is assembled from $\text{Cu}_2(\text{H}_2\text{O})_2$ dimer units and tridentate trimesate (benzene-1,3,5-tricarboxylate) groups to form a three-dimensional framework structure containing a three-dimensional channel system, with channels of pore size 9.5 Å (see Figure S1 in the Supporting Information).

The high-resolution AFM deflection micrographs of the growing {111} face of HKUST-1 as a function of time are shown in Figure 1 (see Figure S2 in the Supporting Information for additional micrographs). The micrograph taken before injection of the growth solution, Figure 1a, reveals a complex surface topography of the substrate HKUST-1 crystal that contains several growth steps, a number of line defects and other gross defect structures.

The crystal face is seen to change drastically after injection of the growth solution with numerous two-dimensional surface nuclei forming all over the crystal surface (Figure 1b). As AFM cannot distinguish between homogeneous and heterogeneous nucleation, we refer to this process as two-dimensional surface nucleation. The lateral dimensions of the two-dimensional nuclei are smaller at the top of Figure 1b than at the bottom indicating growth and spreading of the nuclei during the time taken to scan the crystal surface. Surface islands are visible in Figure 1c indicating that the supersaturation has decreased sufficiently to reduce the rate at which fresh two-dimensional surface nuclei form and so the lateral spread of the previously formed nuclei becomes the more dominant growth process. Subsequent images (Figure 1d and e) reveal further spreading and coalescence of these surface islands and the formation and spreading of new two-dimensional nuclei on existing surface islands. These observations indicate that growth of the crystal surface is through a two-dimensional surface nucleation or “birth and spread” crystal growth mechanism.^[11] Ensuing growth by this mechanism leads to the development of growth hillocks noticeable at the bottom of Figure 1e and which cover almost the entirety of the scanned surface in Figure 1g. Higher resolution images of the large growth hillock marked with an asterisk in Figure 1g (Figure 1h–n) indicate that growth is still proceeding through this crystal growth mechanism at the lowest supersaturation levels of the experiment. Step velocities of ca. 0.4 nm s^{-1} were found at these lower supersaturation levels corresponding to a growth rate perpendicular to the crystal surface of ca. $0.04 \mu\text{m h}^{-1}$. Such step velocities are comparable to those reported in other metal–organic extended solids.^[12] Ultimately, as the supersaturation level drops to zero for crystals allowed to equilibrate with the mother liquor over a period of months surface nucleation ceases. Under these conditions the inherent screw dislocations are exposed which seed a spiral growth front as seen in Figure 2.^[13] Consequently, if crystals were grown at suffi-

[*] M. Shoaee, Prof. M. W. Anderson, Dr. M. P. Attfield
School of Chemistry, The University of Manchester
Brunswick Street, Manchester, M13 9PL (UK)
Fax: (+44) 1612-754-598
E-mail: m.attfield@manchester.ac.uk
Homepage: <http://www.chemistry.manchester.ac.uk/groups/cnm/martin.htm>

[**] We thank the EPSRC and ExxonMobil Research & Engineering for funding and the Royal Society for provision of a University Research Fellowship for M.P.A.

Supporting information for this article is available on the WWW under <http://dx.doi.org/10.1002/anie.200803460>.

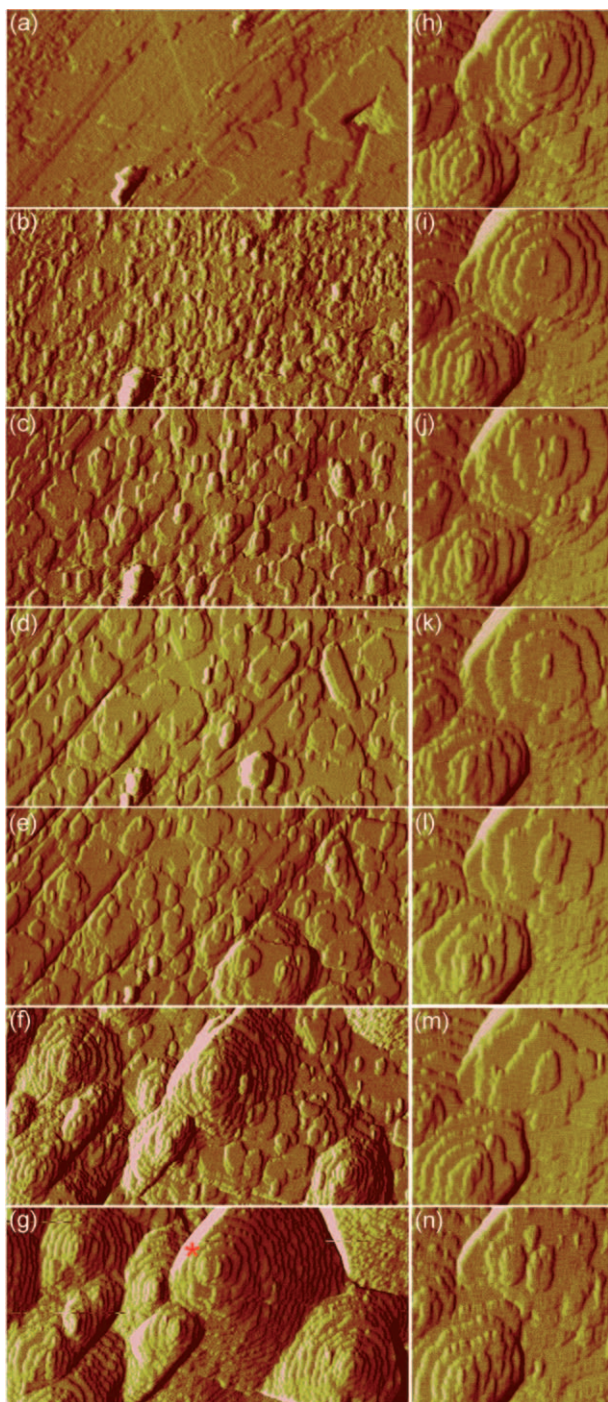


Figure 1. Deflection AFM images of the growing {111} facet of a HKUST-1 crystal after a) 0, b) 4, c) 9, d) 17, e) 31, f) 74, g) 111 h) 123, i) 128, j) 132, k) 137, l) 141, m) 145, n) 154 min. The asterisk in image (g) marks the main growth hillock at the top of images (h)–(n). The image sizes in (a)–(g) and (h)–(n) are $3.0 \times 1.5 \mu\text{m}^2$ and $1.0 \times 1.0 \mu\text{m}^2$, respectively.

ciently low supersaturation, growth can be expected to occur through such a spiral growth mechanism.^[14] At this low level of supersaturation the terraces are also more geometric truncated triangles that adopt the ternary symmetry of the growing {111} face (compare Figure 1 g and Figure 2).

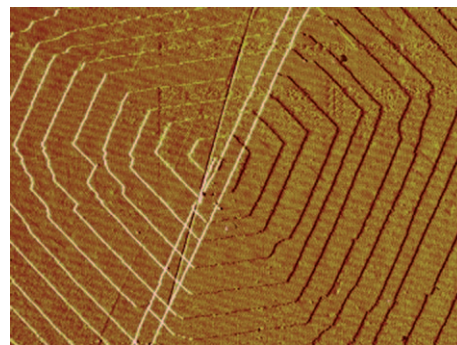


Figure 2. A $4 \times 2.5 \mu\text{m}^2$ ex situ AFM amplitude image of a {111} facet of HKUST-1 showing a growth hillock formed from closed step loops emitted by a pair of non-cooperating growth spirals overlaid with fractures primarily in the $\langle 110 \rangle$ direction.

One aspect of the growth of this crystal surface revealed exclusively by real-time imaging is the influence of line defects present on the initial substrate surface. The line defects, visible as diagonal lines in the bottom left-hand corner of Figure 1 a, initially act as boundaries impeding the step flow of adjacent growing nuclei and islands. This results in the formation of approximately rectangular step bunches, as seen in Figure 1 d and e. Eventually sufficient growth on either side of a line defect enables growth hillocks to form that straddle the area where the line defect was present and the latter is no longer visible as observed in Figure 1 g. Crystal growth over other large gross defects visible on the substrate surface is also evident in Figure 1 a–g. Growth of the crystal surface over these features will introduce defects into the bulk of the resultant crystal that may have beneficial or detrimental effects on its final properties. It is also interesting to note that no fracturing of the newly formed crystal surface is noticeable which supports the observation that the fractures observed in the ex situ AFM images (see Figure 2) of {111} faces of HKUST-1 occur after crystallization.^[13]

Cross-sectional analyses of height images at each time during the growth reveals that the majority of growth steps have heights of $1.5 \pm 0.1 \text{ nm}$ corresponding to the $1.5 \text{ nm } d_{111}$ crystal spacing of the HKUST-1 structure, as shown in Figure 3 a and b, respectively. This, as reported previously,^[13] reveals strongly preferred surface termination at a well-defined structural element indicating that extended structural units are stabilized in HKUST-1. Structure considerations suggest that the surface plane that is likely to terminate these growth steps is that formed by the layer of Cu-centered octahedra and trimesate groups at (A) in Figure 3 b or the CO_2^- groups of the trimesate moieties immediately beneath this layer of octahedra.^[13,15] These growth step heights are consistent with those reported for the ex situ AFM study of HKUST-1 crystals containing surface growth spirals and demonstrate that the same extended structural units are present at the surface of crystals of HKUST-1 grown by a spiral or a two-dimensional surface nucleation crystal growth mechanism. The observation of growth steps corresponding to multiples of the $0.76 \text{ nm } d_{222}$ crystal spacing, for instance with a height of 2.2 nm , indicate that growth steps with less stable surface termination layers are also present on the

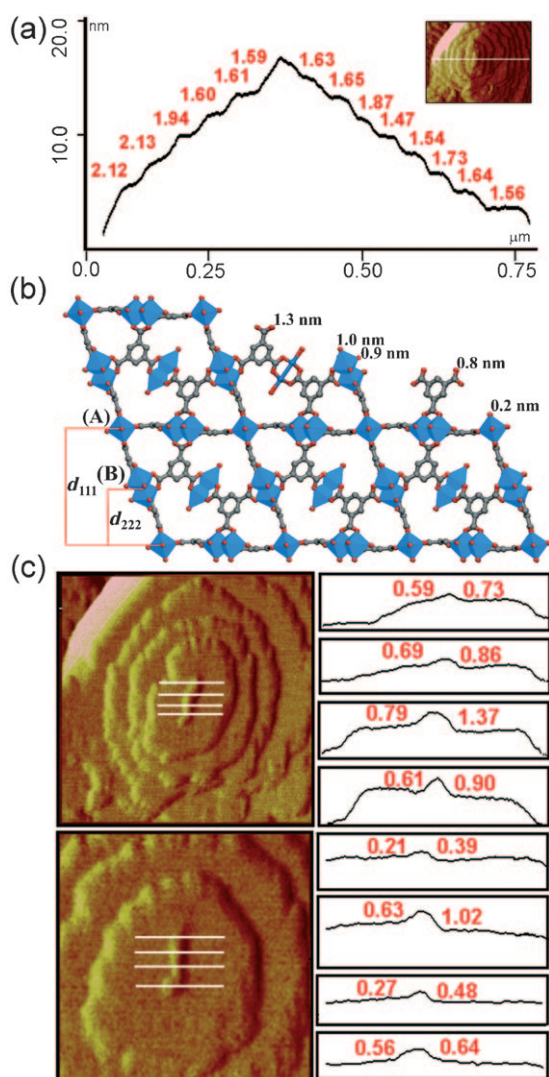


Figure 3. a) Cross-sectional analysis of a typical step train on the {111} face of HKUST-1; b) the structure of HKUST-1 viewed down a <110> direction highlighting possible d_{111} and d_{222} crystal spacings and the perpendicular height of the oxygen atoms of possible intermediate surface terminations above the copper species in the layer (A); c) cross-sectional analyses at various points along different nuclei on the top most layer of a growth hillock. All heights are quoted in nm.

growing crystal surface. The less stable surface plane that is likely to terminate growth steps is that formed by the layer of Cu-centered octahedra at (B) in Figure 3b or the CO_2^- groups of the trimesate moieties immediately beneath this layer of octahedra.^[13,15]

In situ AFM monitoring of crystal growth provides a unique opportunity to observe intermediate structures of the crystal structure formed during the crystal growth process. Cross-sectional analyses of the height images of the freshly formed or growing nuclei on the top most layer of the growth hillocks provide such information about the intermediate structures formed as a stable 1.5 nm layer is constructed. Such analyses reveal a wide range of nuclei heights ranging from 0.2 to 1.5 nm gathered from a variety of the top most nuclei/surface islands in Figure 1. It is also found that the height at

different points along the nuclei can vary within the aforementioned range, as seen in Figure 3c. The heights above the copper species in the layer (A) of the possible intermediate surface terminations at different stages during the growth of a 1.5 nm growth step are shown in Figure 3b. The various plausible height differences that can be envisaged to be occurring during growth of a 1.5 nm growth layer are {0.6, 0.8, 1.1 nm}, {0.4, 1.0, 1.2 nm}, {0.3, 0.7, 1.3 nm} and {0.2, 0.5, 0.9 nm} for the heights above the layer of Cu-centered octahedra at (A), the CO_2^- groups of the trimesate moieties immediately beneath the layer of octahedra at (A), the layer of Cu-centered octahedra at (B) or the CO_2^- groups of the trimesate moieties immediately beneath the layer of octahedra (B), respectively. These height differences encompass the range of heights observed. More specific assignment of the observed heights to the identity of surface attached growth units can not be made as the exact nature of the terminating surface is not known. The range of observed heights suggest that the growth unit of this material is not solely a preformed $\{\text{Cu}_2(\text{H}_2\text{O})_2[\text{H}_{2-n/4}(\text{O}_2\text{C})_3\text{C}_6\text{H}_3]_4\}^{n-}$ paddle wheel-type SBU (see Figure S3 in the Supporting Information) in contrast to the trimeric and dimeric metal carboxylate SBU species that have been identified in solutions close to real crystallisation conditions for two other MOFs.^[5d,e] Simple addition of such a SBU to a layer of Cu-centered octahedra would result only in 1.1 or 1.3 nm step heights being observed. Addition of this SBU at the CO_2^- groups of the trimesate moieties with substitution of at least one of the trimesate groups from the SBU would result in 1.0 nm or 0.5 nm steps heights being observed for addition at the CO_2^- groups of the trimesate moieties immediately beneath the layer of octahedra at (A) or (B), respectively. The former of these two height differences would be expected to be observed predominantly as surface termination at (A) is more stable. Clearly, the observed height differences cover a greater range than these four height differences with many falling below the smallest height difference (1.0 nm) expected for addition of this SBU to the more stable termination layer (A). This indicates that the actual units of growth are more likely to be simpler fragments, such as individual solvated trimesate or Cu^{2+} ions, a trimesate anion with Cu^{2+} cations coordinated to one or more of the CO_2^- groups of the trimesate moiety or perhaps a copper dimer type unit in which the connection of the copper ions is through one or more bridging nitrate groups. An example of the latter has been reported in the crystal structure of $[\text{Cu}_2(\text{C}_{10}\text{H}_7\text{N}_2\text{O})_2(\text{NO}_3)] \cdot \text{H}_2\text{O}$.^[16] The range of observed heights for the different growing nuclei, and on any particular nuclei, result from the nuclei imaged at different stages of addition of these simpler fragments to the growing nuclei on the top most layer of the growth hillocks. The growth of HKUST-1 crystals by simple fragments in this manner is in agreement with work demonstrating that supported films of HKUST-1 are grown in a step-by-step approach by repeated addition of the copper acetate followed by trimesate ions, although whether the copper acetate remains as a copper acetate paddle wheel dimeric SBU during the synthesis was not investigated.^[8]

In conclusion, this work provides the first high-resolution in situ AFM study of the crystal growth of a crystalline

nanoporous material that presents definitive real-time evidence of the crystal growth mechanism, that defects are incorporated into the crystal and insight into the actual units of attachment during the growth of the extended growth layers that exist on the crystal surface of HKUST-1. Such findings will affect how the growth of extended and framework materials is considered, particularly with respect to the fundamental building blocks of growth, and clearly demonstrates the power and potential of in situ AFM to interrogate the crystal growth of crystalline nanoporous and framework materials.

Experimental Section

The substrate crystals of HKUST-1 were prepared as previously described^[13] except that the crystallisation period used was 8 weeks. The crystals were subsequently dried in air at room temperature. Some of these single crystals were set in a Bi:In:Pb:Sn alloy (49:21:18:12 wt %; Alfa Aesar). Atomic force micrographs were recorded on a Veeco Multimode AFM with NanoScope III controller operating in contact mode. Silicon nitride cantilevers with a force constant of 0.06 N m^{-1} were used at a scan rate of 2 Hz. The fluid cell of the AFM was filled with a 0.0011 M growth solution of $\text{Cu}(\text{NO}_3)_2 \cdot 2.5 \text{H}_2\text{O}$ (Aldrich) and trimesic acid (Aldrich) in dimethylformamide (DMF; Aldrich). AFM deflection micrographs of the growing {111} face of a HKUST-1 crystal were recorded as a function of time under this static growth solution. The experiment was conducted at room temperature (ca. 23°C). The precision of the terrace height measurements was determined by measuring at least 20 separate heights and is identical to that determined using the same instrument on other crystal systems.^[4d] The step velocities at the lower supersaturation levels were calculated by tracking the distance traveled by the same step features in two consecutive images and the growth rate perpendicular to the crystal surface was calculated using the method of Frank.^[17,11b]

Received: July 17, 2008

Keywords: atomic force microscopy · crystal growth · HKUST-1 · metal–organic frameworks · microporous materials

- [1] a) P. A. Wright, *Microporous Framework Solids*, Royal Society of Chemistry, Cambridge, **2008**, pp. 1–429; b) M. E. Davis, *Nature* **2002**, *417*, 813–821; c) J. L. C. Rowsell, O. M. Yaghi, *Microporous Mesoporous Mater.* **2004**, *73*, 3–14; d) M. J. Rosseinsky, *Microporous Mesoporous Mater.* **2004**, *73*, 15–30;

- e) S. Kitagawa, R. Kitaura, S. Noro, *Angew. Chem.* **2004**, *116*, 2388–2430; *Angew. Chem. Int. Ed.* **2004**, *43*, 2334–2375.
 [2] M. Kawano, T. Haneda, D. Hashizume, M. Fujita, *Angew. Chem.* **2008**, *120*, 1289–1291; *Angew. Chem. Int. Ed.* **2008**, *47*, 1269–1271.
 [3] a) H. H. Teng, P. M. Dove, J. J. Yoreo, *Geochim. Cosmochim. Acta* **2000**, *64*, 2255–2266; b) R. E. Sours, A. Z. Zellelow, J. A. Swift, *J. Phys. Chem. B* **2005**, *109*, 9989–9995.
 [4] a) M. W. Anderson, J. R. Agger, L. I. Meza, C. B. Chong, C. S. Cundy, *Faraday Discuss.* **2007**, *136*, 143–156; b) P. Q. Miraglia, B. Yilmaz, J. Warzywoda, S. Bazzana, A. Sacco, *Microporous Mesoporous Mater.* **2004**, *69*, 71–76; c) S. Yamamoto, S. Sugiyama, O. Matsuoka, K. Kohmura, T. Honda, Y. Banno, H. Nozoye, *J. Phys. Chem.* **1996**, *100*, 18474–18482; d) L. I. Meza, M. W. Anderson, J. R. Agger, *Chem. Commun.* **2007**, 2473–2475.
 [5] a) G. Ferey, *J. Solid State Chem.* **2000**, *152*, 37–48; b) F. Taulelle, *Curr. Opin. Solid State Mater. Sci.* **2001**, *5*, 397–405; c) A. Ramanan, M. S. Whittingham, *Cryst. Growth Des.* **2006**, *6*, 2419–2421; d) S. Surblé, F. Milange, C. Serre, G. Ferey, R. J. Walton, *Chem. Commun.* **2006**, 1518–1520; e) J. A. Rood, W. C. Bogge, B. C. Noll, K. W. Henderson, *J. Am. Chem. Soc.* **2007**, *129*, 13675–13682.
 [6] S. S. Y. Chui, S. M. F. Lo, J. P. H. Charmant, A. G. Orpen, I. D. Williams, *Science* **1999**, *283*, 1148–1150.
 [7] E. Biemmi, C. Scherb, T. Bein, *J. Am. Chem. Soc.* **2007**, *129*, 8054–8055.
 [8] O. Shekhah, H. Wang, S. Kowarik, F. Schreiber, M. Paulus, M. Tolan, C. Sternemann, F. Evers, D. Zacher, R. A. Fischer, C. Woll, *J. Am. Chem. Soc.* **2007**, *129*, 15118–15119.
 [9] U. Mueller, M. Schubert, F. Teich, H. Puetter, K. Schierle-Arndt, J. Pastré, *J. Mater. Chem.* **2006**, *16*, 626–636.
 [10] B. Xiao, P. S. Wheatley, X. B. Zhao, A. J. Fletcher, S. Fox, A. G. Rossi, I. L. Megson, S. Bordiga, L. Regli, K. M. Thomas, R. E. Morris, *J. Am. Chem. Soc.* **2007**, *129*, 1203–1209.
 [11] a) M. Volmer, *Kinetik der Phasenbildung*, Steinkopff, Leipzig, **1939**; b) J. W. Mullin, *Crystallization*, Butterworth Heinemann, Oxford, **2001**, pp. 216–288.
 [12] K. Wang, D. Sun, J. Zhang, W. Yu, H. Liu, X. Hu, S. Guo, Y. Geng, *J. Cryst. Growth* **2004**, *261*, 63–69.
 [13] M. Shoaee, J. R. Agger, M. W. Anderson, M. P. Attfield, *CrystEngComm* **2008**, *10*, 646–648.
 [14] K. Sangwal, *Prog. Cryst. Growth Charact.* **1998**, *36*, 163–248.
 [15] A. M. Walker, B. Slater, *CrystEngComm* **2008**, *10*, 790–791.
 [16] J. P. Zhang, Z. B. Han, X. M. Chen, *Chin. J. Inorg. Chem.* **2004**, *20*, 1213–1215.
 [17] F. C. Frank in *Growth and Perfection of Crystals* (Eds.: R. H. Doremus, B. W. Roberts, D. Turnbull), Wiley, New York, **1958**, pp. 411–420.